JOURNAL OF GEOPHYSICAL RESEARCH, VOL. 105, NO. A11, PAGES 24,889–24,898, NOVEMBER 1, 2000

A plasma vortex revisited: The importance of including ionospheric conductivity measurements

M. J. Kosch
Max-Planck-Institut für Aeronomie, Katlenburg-Lindau, Germany

O. Amm
Finnish Meteorological Institute, Helsinki, Finland

M. W. J. Scourfield
Space Physics Research Institute, University of Natal, Durban, South Africa

Abstract. In an earlier paper [*Kosch et al*., 1998], simultaneous all-sky TV imager and Scandinavian Twin Auroral Radar Experiment (STARE) observations of an ionospheric plasma vortex located poleward of an auroral arc were presented. The vortex is associated with a sudden brightening of the arc and corresponds to an ionospheric region of diverging horizontal electric fields, which is equivalent to a downward field-aligned current (FAC), i.e., the closure current for the upward current above the arc. This event has been revisited because of the subsequent availability of data from the Scandinavian Magnetometer Array. These data, combined with STARE electric fields, have been used to determine the real ionospheric conductance distribution throughout the field of view. As a result, a more realistic, quantitative picture of the current system associated with the arc is obtained than was possible in an earlier model based on an assumed constant conductance. In particular, a complete macroscopic electrodynamic description of a plasma vortex, composed of ionospheric conductances, true horizontal currents, and FACs, is obtained for the first time. It is shown that the plasma vortex corresponds to an area of decreased conductance, thus broadening the FAC distribution and reducing the current density compared to the earlier results. The study illustrates that horizontal conductance gradients should not be neglected when computing FACs.

1. Introduction

The precipitation of energetic particles in, for example, auroral arcs can result in small-scale longitudinal and latitudinal conductivity gradients. Such conductivity gradients, which can also be highly variable in time, occur within localized regions of as little as 1–20 km, the width of auroral arcs. Strong conductivity gradients modify the convection-driven electrojets and the associated convection electric fields. Measurements of electric fields, currents, and conductivities for a localized region of 20 km or less are rather difficult for satellite, rocket, and most ground-based experiments. A concise summary of the various relationships that have been found to exist between electric fields and conductivities, in association with auroral arcs, is given by *Aikio et al*. [1993], *Marklund* [1984], and *Baumjohann* [1983].

There have been numerous observations [*Evans et al*., 1977; *Horwitz et al*., 1978; *Cahill et al*., 1980; *Stiles et al*., 1980; *de la Beaujardiere et al*., 1981; *Marklund et al*., 1982; *Ziesolleck et al*., 1983; *Brüning and Goertz*, 1986; *Timofeev et al*., 1987; *Opgenoorth et al*., 1990; *Valladares and Carlson*, 1991; *Aikio et al*., 1993; *Lewis et al*., 1994] of enhanced electric fields equatorward (poleward) of an arc in the premidnight (postmidnight) sector. In fact, this is a common feature of arcs at all local times [*Opgenoorth et al*., 1990]. Such regions of electric fields have been referred to as a "radar arc" because coherent radar backscatter also occurs there. *Timofeev et al*. [1987] found that postmidnight radar arcs appear, or suddenly intensify, with the optical brightening of the associated auroral arc.

Aikio et al. [1993] have proposed the following scenario based on satellite measurements. A current system associated with auroral arcs consists of a matched pair of magnetic field-aligned currents (FACs). The upward current flowing above the arc and the downward return current flowing on the poleward (equatorward) side of the arc in the postmidnight (premidnight) sector are connected by a Pedersen current in the ionosphere. Since the Pedersen current will flow in the direction of the convection electric field (equatorward postmidnight and poleward premidnight), this determines on which side of the optical arc the radar arc is observed. The upward current is carried by the energetic precipitating electrons responsible for the auroral arc. The downward current is carried by upward fluxes of low-energy ionospheric electrons outside of the arc, resulting in a depletion of ionospheric conductivity in that region. If the magnetospheric process resulting in an auroral arc acts as a current generator, then the ionospheric electric field has to modify itself in such a way that current continuity in the ionosphere is preserved. Therefore the meridional electric field has to increase, in conjunction with an enhanced ionospheric Pedersen current, in order to support the enhanced downward current due to the increased upward current above the arc. *Tsunoda et al*. [1976] and *Timofeev et al*.

Paper number 2000JA900102.
0148-0227/00/2000JA900102$09.00

[1987] have shown that the radar aurora corresponds to downward FACs linked to the visual aurora by an ionospheric Pedersen current.

Normally, it is difficult to make a quantitative analysis of the FACs, as there is no simple way to estimate the ionospheric conductivity distribution, or the particle flux, corresponding to the auroral arc. For the event under study here, the European Incoherent Scatter facility (EISCAT) [*Folkestad et al*., 1983] was not available, and the TV images were not calibrated in intensity or wavelength. However, two other experiments with overlapping fields of view were available: the Scandinavian Twin Auroral Radar Experiment (STARE) [*Greenwald et al*., 1978] for ionospheric plasma flows and electric fields and the Scandinavian Magnetometer Array (SMA) [*Küppers et al*., 1979] for geomagnetic field disturbances and the corresponding equivalent currents. STARE is sensitive to electrostatic waves in the auroral E layer at ~105 km altitude [*Fejer and Kelley*, 1980]. The mean Doppler shift of these waves is used to deduce good approximations of the speed and direction of the electron Hall drift. This method gives two-dimensional maps of the plasma flow, and hence the electric field, over a section of the auroral oval at those locations where the ionospheric electric field exceeds a threshold of ~15 mV/m [*Cahill et al*., 1978]. The measurements are made with good spatial resolution (20 × 20 km) over a large area (500 × 500 km) and are carried out on a continuous basis with a time resolution of 10 s. The SMA consists of a two-dimensional array of 36 magnetometers located throughout much of Scandinavia and Finland [*Küppers et al*., 1979]. Within STARE's field of view (67.6°–72.6°N, 13.5°–26.0°E) the array density maximizes with magnetometers located on a grid of about 120 × 120 km. The SMA was designed to operate continuously, with a time resolution of 10 s, throughout the International Magnetometer Study period of 1977–1979. Extensive auroral substorm studies have been undertaken, partly including STARE [*Untiedt and Baumjohann*, 1993]. At the time of the event studied here (January 15, 1980), not all of the stations were operational. However, some 13 stations within STARE's field of view, and just beyond the periphery, continued recording.

Since the ground magnetic field disturbance depends on the height-integrated horizontal ionospheric current density **J**, and because the ionospheric electric field **E** is connected to **J** by Ohm's law via the Hall (Σ_H) and Pedersen (Σ_P) height-integrated conductivities, it is possible to estimate the two-dimensional conductance distribution of the ionosphere if the two-dimensional equivalent current $\mathbf{J}_{eq}$ and **E** distributions are known [*Baumjohann et al*., 1981; *Inhester et al*., 1981; *Opgenoorth et al*., 1983a, 1983b]. For northern Scandinavia, both $\mathbf{J}_{eq}$ and **E** are known from measurements in the overlapping fields of view of STARE and the SMA. *Inhester et al*. [1992] showed that, in many cases, this was uniquely possible with an estimate of the Hall to Pedersen conductance ratio α, which can be assessed using either optical [*Mende et al*., 1984; *Robinson et al*., 1989] or ground magnetic data [*Vickrey et al*., 1981; *Schlegel*, 1988; *Lester et al*., 1996]. If α is measured locally by the EISCAT radar, even this assumption need no longer be necessary. *Amm* [1995] has implemented the concept of *Inhester et al*. [1992], called "method of characteristics," into a computerized algorithm and extended it to spherical coordinates [*Amm*, 1998]. Using the 13 SMA stations still operating within or near STARE's field of view at the time of the event, it has been possible to reconstruct a realistic three-dimensional current system associated with the event discussed in this paper.

We derive the equation for FACs in the ionosphere to illustrate the importance of conductance gradients. Ohm's law in the ionosphere is

$$\mathbf{J} = \Sigma_P \mathbf{E} + \Sigma_H(\hat{\mathbf{B}} \times \mathbf{E}), \tag{1}$$

where **J** is the current vector, **E** the electric field vector, Σ_P and Σ_H are the height-integrated Pedersen and Hall conductivities, respectively, and $\hat{\mathbf{B}}$ is the unit vector in the direction of the Earth's magnetic field.

Assuming a vertical magnetic field with $\hat{\mathbf{B}}$ pointing along the Z axis, $\hat{\mathbf{z}}$ being the unit vector pointing downward, the FAC is given by

$$J_\parallel = \text{div}\,\mathbf{J} = \text{div}\,(\Sigma_P \mathbf{E}) + \text{div}\,[\Sigma_H\,(\hat{\mathbf{z}} \times \mathbf{E})]. \tag{2}$$

Expanding (2),

$$J_\parallel = \Sigma_P\,\text{div}\,\mathbf{E} + \nabla\Sigma_P \cdot \mathbf{E} + \nabla\Sigma_H \cdot (\hat{\mathbf{z}} \times \mathbf{E}) + \Sigma_H\,\text{div}\,(\hat{\mathbf{z}} \times \mathbf{E}). \tag{3}$$

The last term of (3) is zero because

$$\text{div}\,(\hat{\mathbf{z}} \times \mathbf{E}) = \mathbf{E} \cdot \text{rot}(\hat{\mathbf{z}}) - \hat{\mathbf{z}} \cdot \text{rot}(\mathbf{E}),$$

where $\mathbf{E} \cdot \text{rot}(\hat{\mathbf{z}}) = 0$ by definition and $\hat{\mathbf{z}} \cdot \text{rot}(\mathbf{E}) = 0$ since we assume that a curl-free potential electric field exists in the ionosphere. Hence

$$J_\parallel = \Sigma_P\,\text{div}\,\mathbf{E} + \nabla\Sigma_P \cdot \mathbf{E} + \nabla\Sigma_H \cdot (\hat{\mathbf{z}} \times \mathbf{E}). \tag{4}$$

It is clear that assuming uniform conductances (i.e., dropping the last two terms of (4)) may lead to considerable errors in computing FACs, since the terms relating to the conductance gradients are of the same order, often larger, and can be of opposite sign to the first term in (4). In some studies [e.g., *Sofko et al*., 1995; *Sato et al*., 1995] the first term was named "magnetospheric FAC," while the remaining terms were named "ionospheric FAC" by these authors. However, in the coupled magnetosphere-ionosphere system, such a subdivision is not reasonable since ionospheric conductance gradients are the consequence of magnetospheric processes, as in the present study. The last two terms of (4) were also omitted, with significant consequences, in the previous study of the event revisited here [*Kosch et al*., 1998].

Any ionospheric current measurement from ground-based magnetometers will include a component due to the motion of the neutral thermosphere. The neutral dynamo effect can be expressed in the following way:

$$\mathbf{E} = (\mathbf{u} - \mathbf{v}) \times \hat{\mathbf{B}}, \tag{5}$$

where **u** is the neutral wind vector and **v** the ion flow vector.

The current vector **J** is affected by the neutral motion via (1). Clearly, the neutral wind opposes the ion flow and hence reduces the effective electric field. Since thermospheric neutral forcing is ion drag dominated [*Killeen and Roble*, 1984], the neutral wind speed shows a clear relationship with geomagnetic indices such as *Kp* or *AE* [*McCormac et al*., 1987; *Aruliah et al*., 1991]. Generally, thermospheric neutral motion follows the ion convection pattern [*Killeen and Roble*, 1988, and references therein] with an e-folding delay time of 1–3 hours [*Killeen et al*., 1984]. Neutral winds can be measured by ground-based optical interferometers in the lower and upper thermosphere using the Doppler shift of the O^1S 557.7 and O^1D 630 nm auroral emission lines [*Kosch et al*., 2000]. Although electric field measurements by an incoherent backscatter radar,

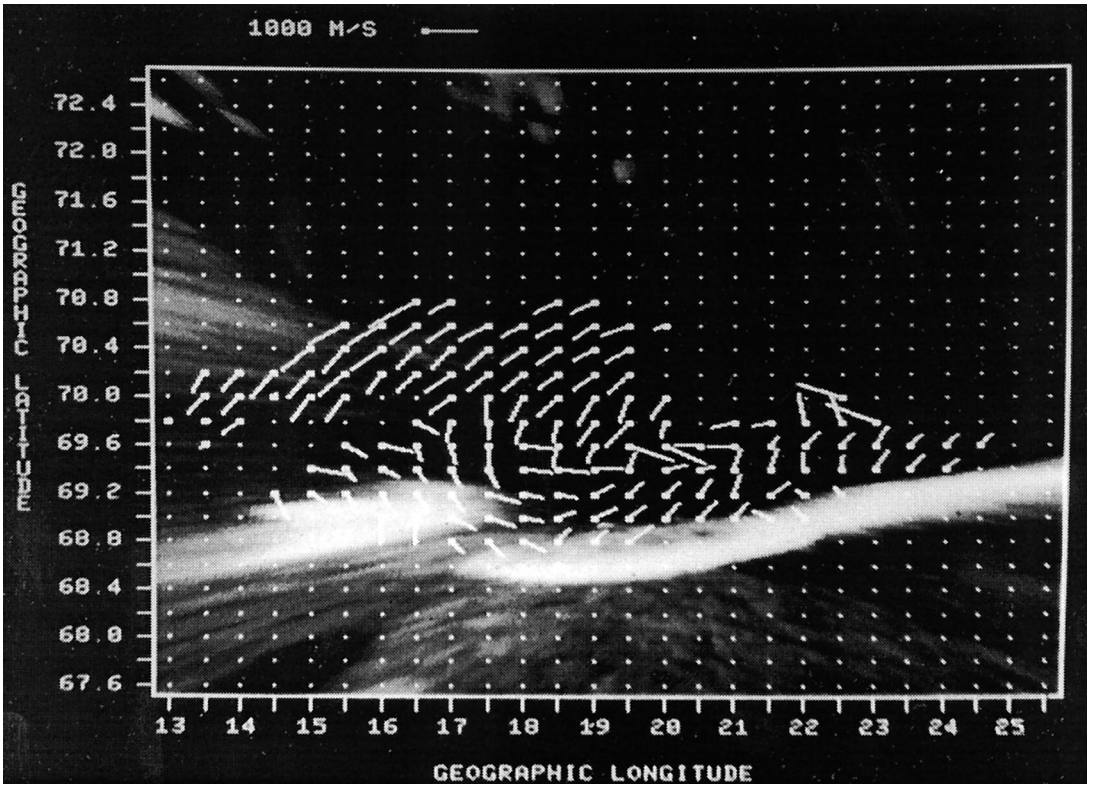

Figure 1. The white-light TV image of the east-west aligned arc after it had brightened, taken at 2135 UT on January 15, 1980. The all-sky image has been mapped onto a rectilinear geographic grid, at an altitude of 100 km, to remove the all-sky distortion. Superimposed is a grid of Scandinavian Twin Auroral Radar Experiment (STARE) plasma flow vectors, with the direction pointing away from each white dot. Locations with no vectors correspond to no radar backscatter.

such as EISCAT [*Folkestad et al*., 1983], would be affected by neutral winds because it measures ion flow directly, a coherent backscatter radar such as STARE is not. This is because STARE infers the electric field by indirectly measuring the electron Hall drift, as explained earlier, which is not affected by neutral winds.

2. Observations and Discussion

The results reported here were obtained by three high-resolution systems with overlapping fields of view: a low light level TV camera for optical imaging, the Scandinavian Twin Auroral Radar Experiment (STARE) [*Greenwald et al*., 1978] for ionospheric plasma flows and electric fields, and the Scandinavian Magnetometer Array (SMA) [*Küppers et al*., 1979] for geomagnetic field disturbances and equivalent currents. Although the event has been described in detail by *Kosch et al*. [1998], it will now be summarized to serve as background for the new work.

The data examined here were obtained at 2135 UT on January 15, 1980, after the Harang discontinuity that occurred at ~2000 UT [*Kosch et al*., 1998]. Geomagnetic conditions were quiet with $\Sigma Kp = 12^-$ on this day and $Kp = 1^+$ for the period 2100–2400 UT, unusually low values for the auroral activity observed. GEOS-2 satellite magnetometer and particle data [*Korth et al*., 1978], obtained at geostationary orbit along the Swedish meridian, show virtually no activity [*Kosch et al*., 1998]. An arc was imaged in white light by an all-sky low-light-level TV camera system operated from Skibotn (69.35°N, 20.36°E, $L = 6$), Norway. Simultaneously, STARE was observing the ionospheric plasma flows within the TV imager's field of view with a 10 s temporal resolution and 20 × 20 km spatial resolution. The SMA was recording the ground magnetic disturbance due to ionospheric currents, again with 10 s temporal resolution. At 2134 UT a surge of luminosity propagated eastward along the arc at ~4 km/s, causing enhanced brightness and some distortion of the arc. It was during the enhanced brightening of the arc, which attained its maximum 1 min later, that a counterclockwise plasma vortex was observed by STARE. Simultaneously, a clockwise vortex in equivalent current was observed in the SMA data.

Figure 1 shows a mapping of the auroral image, reproduced from *Kosch et al*. [1998], recorded at 2135 UT onto a rectilinear geographic grid, for an altitude of 100 km, to remove the all-sky spatial distortion. The apparent radial streaking in the image near the edges is partially due to the vertical extent of the aurora. The thickness of the arc is ~20 km. Superimposed is the grid of STARE *E* region plasma flow vectors with the direction pointing away from each white dot. Locations with no vectors correspond to no radar backscatter. The radar data projection is also for 100 km altitude. The patch of luminosity near the southwest horizon is an artifact of artificial illumination. A counterclockwise plasma vortex is visible centered between 17° and 21° longitude and covers a region of about 180 × 140 km in spatial extent. Westward drifts at higher latitudes merge with eastward drifts at lower latitudes near the arc. The plasma vortex drifted eastward at about 700–800 m/s and is

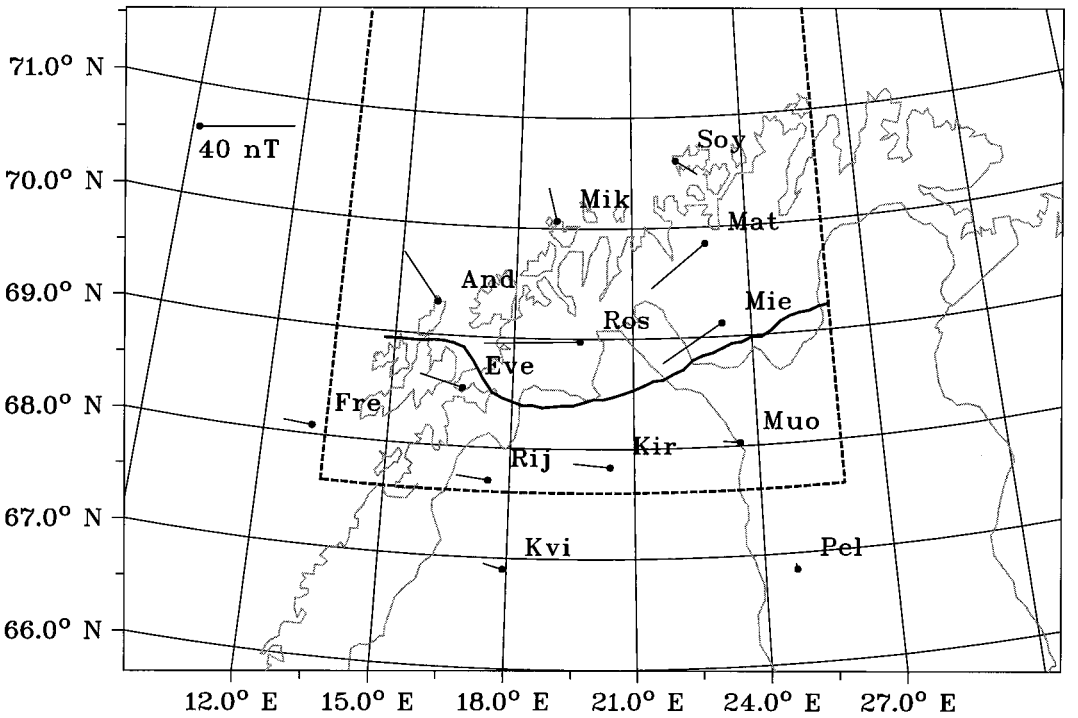

Figure 2. A map of northern Scandinavia showing the Scandinavian Twin Auroral Radar Experiment (STARE) field of view (dashed line), the locus of maximum auroral intensity (solid curve), and the location of the Scandinavian Magnetometer Array (SMA) stations used in the study (dots). The vectors, with the direction pointing away from each dot, are the ground magnetic field disturbance rotated clockwise by 90°. The time is 2135 UT on January 15, 1980.

associated with a moving distortion in the arc in the same range of longitudes. No radar backscatter was observed in the far poleward part of the STARE field of view or anywhere within or equatorward of the arc, indicating ionospheric electric fields below the 15 mV/m threshold [*Cahill et al*., 1978].

Given the very quiet geomagnetic conditions prevailing ($Kp = 1^+$) and that the convection electric field is frequently below the STARE detection threshold in the vicinity of the Harang discontinuity [*Nielsen and Greenwald*, 1979], this indicates that the observed plasma vortex is probably entirely due to mechanisms associated solely with the arc. The appearance of the plasma vortex at the same time as the sudden brightening of the auroral arc, together with the fact that the drifting plasma vortex coincided with a distortion of the arc moving at the same speed, is strong evidence that the vortex is causally related to the activation of the arc [*Kosch et al*., 1998]. *Timofeev et al*. [1987] show several examples of the appearance or intensification of a radar aurora associated with the brightening of a postmidnight auroral arc, consistent with our observation.

Figure 2 shows a map of northern Scandinavia and Finland with the field of view of STARE (dashed line), the lower border of the auroral arc at 2135 UT on January 15, 1980 (solid curve), and the location of each of the SMA stations (dots) used in this study. The thickness of the arc (~20 km) is equivalent to 0.2° in latitude extending southward. Table 1 gives a list of the relevant SMA stations, including full names and geographic locations. The vectors, with the direction pointing away from each SMA station, are the observed horizontal magnetic field disturbance rotated clockwise by 90°. Clearly, even the raw magnetometer data indicate a clockwise vortex structure in equivalent current, which is consistent with the STARE observation shown in Figure 1. The general direction of the current vectors, except for SOY and possibly MIK in the extreme north of the SMA, shows that northern Scandinavia is under the westward electrojet and confirms that the event time is after the Harang discontinuity [*Kosch et al*., 1998].

Figure 3 shows a stack plot of the raw magnetograms for the SMA stations shown in Figure 2 and listed in Table 1. The X (north), Y (east), and Z (vertical down) traces are given in geographic coordinates by the solid, dashed, and dotted curves, respectively, for 2100–2200 UT on January 15, 1980. The time of the event is indicated by the vertical bar. The entire hour shown is a period of low geomagnetic activity with no component deflection exceeding 75 nT. ROS, which is very close to

Table 1. Table of Scandinavian Magnetometer Array Stations Used in This Study

Station	Geographic Latitude, deg	Geographic Longitude, deg
Fredvang (FRE)	68.08	13.17
Andenes (AND)	69.30	16.02
Evenes (EVE)	68.53	16.77
Ritsemjokk (RIJ)	67.70	17.50
Kvikkjokk (KVI)	66.90	17.92
Mikkelvik (MIK)	70.07	19.03
Rostadalen (ROS)	68.97	19.67
Kiruna (KIR)	67.73	20.42
Söröya (SOY)	70.60	22.22
Mattisdalen (MAT)	69.85	22.92
Mieron (MIE)	69.12	23.27
Muonio (MUO)	68.03	23.57
Pello (PEL)	66.85	24.73

Skibotn near the center of STARE's field of view, shows the maximum horizontal magnetic deflection. Other stations in the latitude range 69°–70° poleward of the arc (AND, MAT, and MIE) also show moderate disturbances. Equatorward of the arc (~68.5°N) and poleward of 70°N the magnetic disturbance declines markedly, indicating the localized nature of the event. Fortuitously, both the STARE and SMA signatures of the event maximize above Skibotn during the optical recordings. It seems likely that the ground-based identification of the event associated with the arc required a background of prevailing quiet geomagnetic conditions ($Kp = 1^+$) together with close proximity to the Harang discontinuity. Under active or normal background convection electric field conditions, the vortex signature may have been impossible to identify in the STARE and SMA data.

Instantaneous spatial distributions of the ionospheric macroscopic electrodynamic parameters for 2135 UT on January 15, 1980, are derived using the method of characteristics [*Inhester et al*., 1992; *Amm*, 1995, 1998]. If two-dimensional input data of the ionospheric electric field and the ground magnetic disturbance field are given, this method can infer distributions of ionospheric conductances, actual (not equivalent) ionospheric currents, and magnetic field-aligned currents (FACs). Besides the data, only an approximation of the Hall to Pedersen conductance ratio α has to be provided. This ratio can be modeled by following statistical studies that show its close relation to the general level of ground magnetic activity [*Vickrey et al*., 1981; *Schlegel*, 1988; *Lester et al*., 1996]. Only a rough estimate of α is needed, since the influence of the ratio on the final results has been shown to be uncritical [*Amm*, 1995]. For this study, the most realistic Hall to Pedersen conductance ratio is taken to be 1.1, in correspondance with $Kp = 1^+$ [cf. *Schlegel*, 1988]. Another computation has been done for $\alpha = 2$, which showed no significant differences, as expected. After extraction of the part of the ground magnetic disturbance field caused by external sources and its field continuation to the ionosphere, a two-dimensional partial differential equation, derived from Ohm's law and the current continuity condition in the ionosphere, is solved along its characteristics to obtain the Hall conductance as a primary output. From this, together with the input data, the remaining ionospheric electrodynamic quantities mentioned above can be inferred (for details, see *Amm* [1998]).

The advantages of this method, compared to other methods that derive ionospheric electrodynamic parameters from ground-based observations, are that the number of modeled input parameters is reduced as much as possible, no uniformity of the conductances has to be assumed (as was the case in the original study of this event [*Kosch et al*., 1998]), and an error estimation is built into the method to obtain information on the uniqueness and existence of the solution. Additionally, only data from the period to be analyzed are needed, i.e., no merging of data from different intervals is required. In contrast, earlier methods that used "composite vector plots" of the input data fields from different time intervals had to assume the movement of a stationary pattern with constant velocity. In particular, the method of characteristics has proven to be much faster and provides more reliable and detailed results than the "trial and error" method [*Baumjohann et al*., 1981; *Inhester et al*., 1981; *Opgenoorth et al*., 1983a, 1983b]. In this study, a spatial grid of 0.5° latitude by 2° longitude, corresponding to about 50 × 80 km, respectively, has been used. For the interpolation of the data onto a regular grid, including some extrapolation of the ground magnetic data, the spherical elementary current systems (SECS) method is used [*Amm and Viljanen*, 1999]. It makes use of the fact that the equivalent currents are divergence-free and that the ionospheric electric field is assumed to be curl-free, thereby preserving these features in the interpolated vector fields.

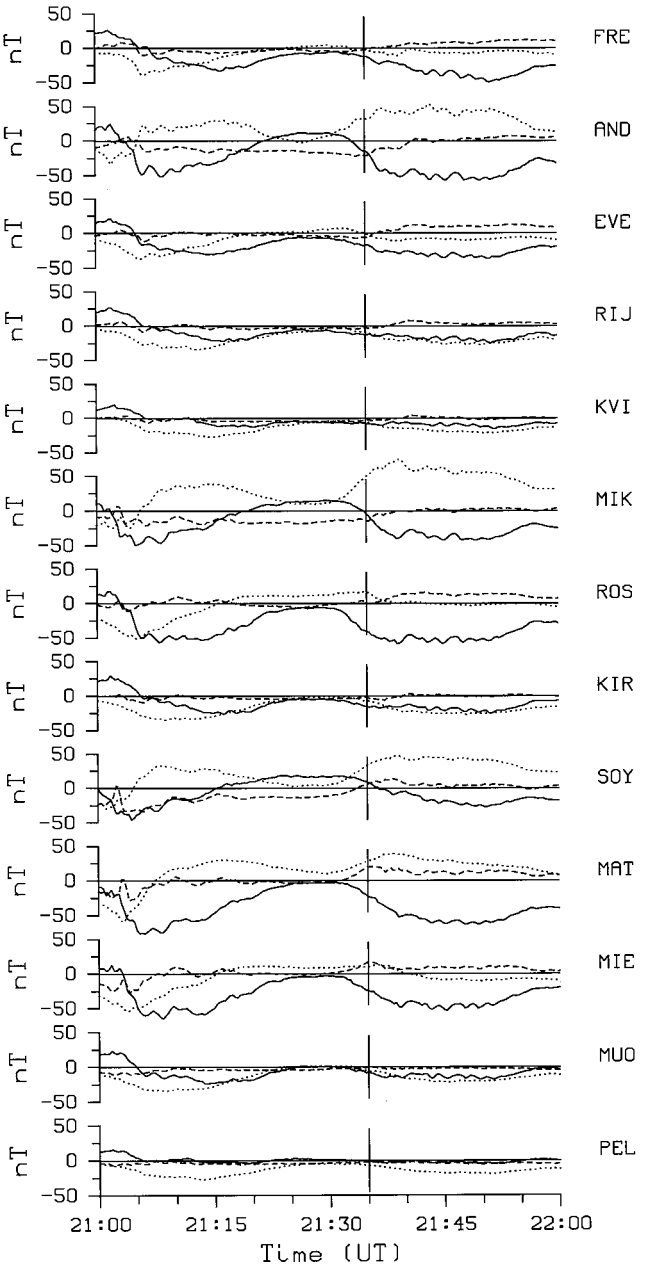

Figure 3. A stack plot showing 1 hour of magnetic traces for the 13 Scandinavian Magnetometer Array (SMA) stations used in the study (see Figure 2). The X (north), Y (east), and Z (vertical down) components are shown as solid, dashed, and dotted curves, respectively, for geographic coordinates. The event occurred at 2135 UT on January 15, 1980.

Applying the method of characteristics, Figure 4a shows the total ionospheric horizontal current distribution in geographic coordinates at 2135 UT on January 15, 1980. The lower border of the arc, projected at 100 km altitude, is also shown. It must be emphasized that the vectors represent real and not equiv-

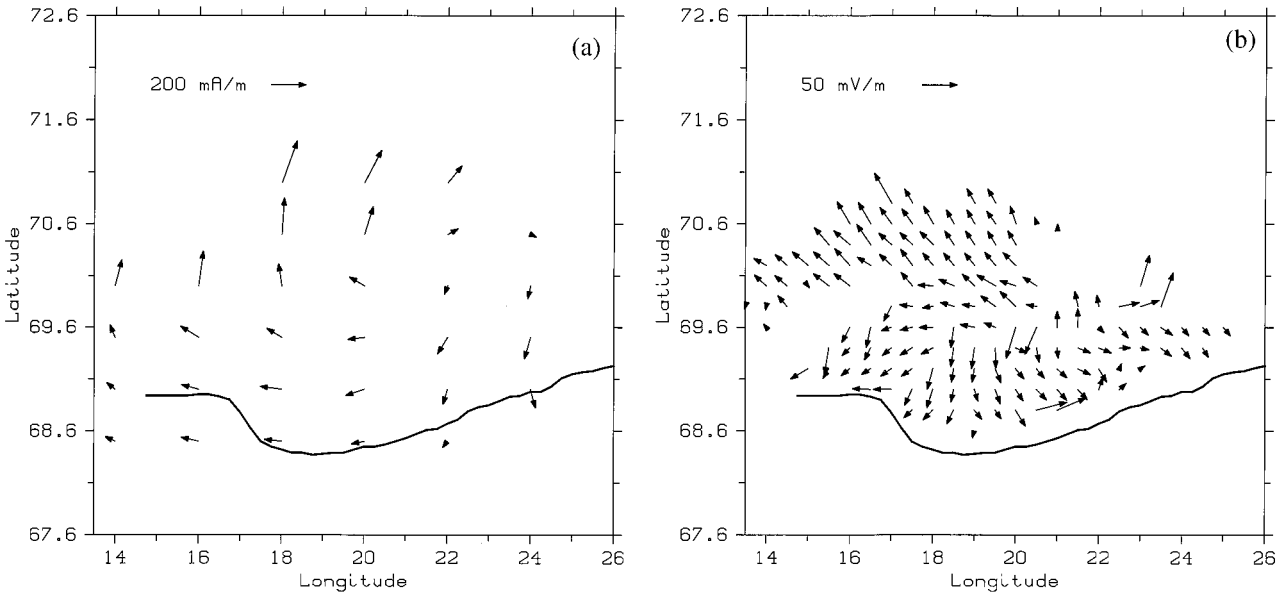

Figure 4. (a) Total horizontal ionospheric current and (b) electric field distributions at 2135 UT on January 15, 1980, in geographic coordinates. The lower border of the arc, projected at 100 km altitude, is also shown.

alent currents. Comparing Figure 4a with Figure 1, it is clear that the clockwise current vortex corresponds closely to the counterclockwise plasma vortex. The effect of any neutral winds (see equations (5) and (1)) has been neglected, as no direct observations are available. This is justified since long-term studies from Kiruna (~150 km south of Skibotn) [*Aruliah et al*., 1991] and recent measurements from Skibotn [*Cierpka et al*., 2000; *Kosch et al*., 2000], using Fabry-Perot interferometers, have shown that the meridional neutral wind speed is <100 m/s for $Kp < 2$, which is similar to the event studied here. The zonal wind speed for the time under study is close to zero. Such wind speeds correspond to an electric field of 5 mV/m, which is small in comparison to the measured electric fields discussed below (see Figure 4b).

E region plasma flow drifts observed by coherent-backscatter radar may be converted into equivalent ionospheric horizontal electric fields by rotating the vector clockwise through 90° and setting 1000 m/s ≈ 50 mV/m ($\mathbf{V} = \mathbf{E} \times \mathbf{B}$). Using this transform, Figure 4b shows the ionospheric horizontal electric field distribution, corresponding to the drift velocity shown in Figure 1, in exactly the same format as Figure 4a. No compensation for neutral winds is necessary here, as discussed earlier. In Figure 4b the electric field vectors near the arc, corresponding to eastward plasma flow (see Figure 1), point approximately toward the arc. This result is not unexpected, as it indicates a horizontal ionospheric current flowing into the arc, which is necessary to feed the upward FAC normally present in arcs [*Armstrong et al*., 1975; *Kamide and Akasofu*, 1976a, 1976b; *de la Beaujardiere et al*., 1977; *Evans et al*., 1977; *Cahill et al*., 1980; *Robinson et al*., 1981; *Marklund et al*., 1982; *Brüning and Goertz*, 1986]. *Aikio et al*. [1993] and *Timofeev et al*. [1987] have shown examples of the electric field enhancement adjacent to an auroral arc being simultaneous with the optical brightening of the arc. These are consistent with our observation. The electric fields north of the arc, corresponding to westward plasma flow (see Figure 1), point approximately away from the arc. This is indicative of a downward FAC in the region around 69.6°N, where the electric field reverses, consistent with the divergence of the electric field. The region of electric field divergence, centered approximately on 69.6°N and 21°E, also corresponds with the center of the horizontal current vortex. Since the Pedersen currents flow parallel to the electric field, they are the main carrier of current between the downward FACs in the vortex and the upward FACs in the arc. However, Pedersen currents and their associated FACs together produce a nearly vanishing magnetic field below the ionosphere [*Fukushima*, 1976; cf. *Amm*, 1997]. Thus the ground magnetic effect is dominated by the Hall currents circulating clockwise around the vortex (see Figure 4a).

Knowledge of the ionospheric conductivity is essential for computing realistic FACs. In the original study of this event [*Kosch et al*., 1998] it had not been possible to make a realistic estimate of the ionospheric conductance distribution. For simplicity and on the basis of the low geomagnetic activity ($Kp = 1^+$), a uniform Pedersen conductance of 1 S was assumed. This major limitation has now been removed by using the method of characteristics [*Amm*, 1998]. Figure 5a shows the quantitative Hall height-integrated conductivity distribution at 2135 UT on January 15, 1980, in geographic coordinates. The lower border of the arc, projected at 100 km altitude, is also shown together with conductance contours plotted in siemens. Clearly, the values of conductance are considerably higher than unity. Furthermore, the Hall conductance varies from 4.5 to 8.5 S, a variation of almost a factor of 2, in marked contrast to a spatially uniform conductance of unity assumed in the original study [*Kosch et al*., 1998]. It is this latter point that has a most significant effect on the FACs, as will be discussed below. It is seen that the conductance measurement reproduces the arc rather well except near the ends of the arc. The mismatch is due to the vertical extent of the arc which is mapped to the incorrect horizontal position near the edges of the field of view, edge effects in the method of characteristics resulting from a lack of SMA stations around the periphery of the field of view, and the absence of STARE backscatter equatorward of the arc. Considering the thickness of the arc (~20 km) and the spacing of the SMA stations (~120 km), the

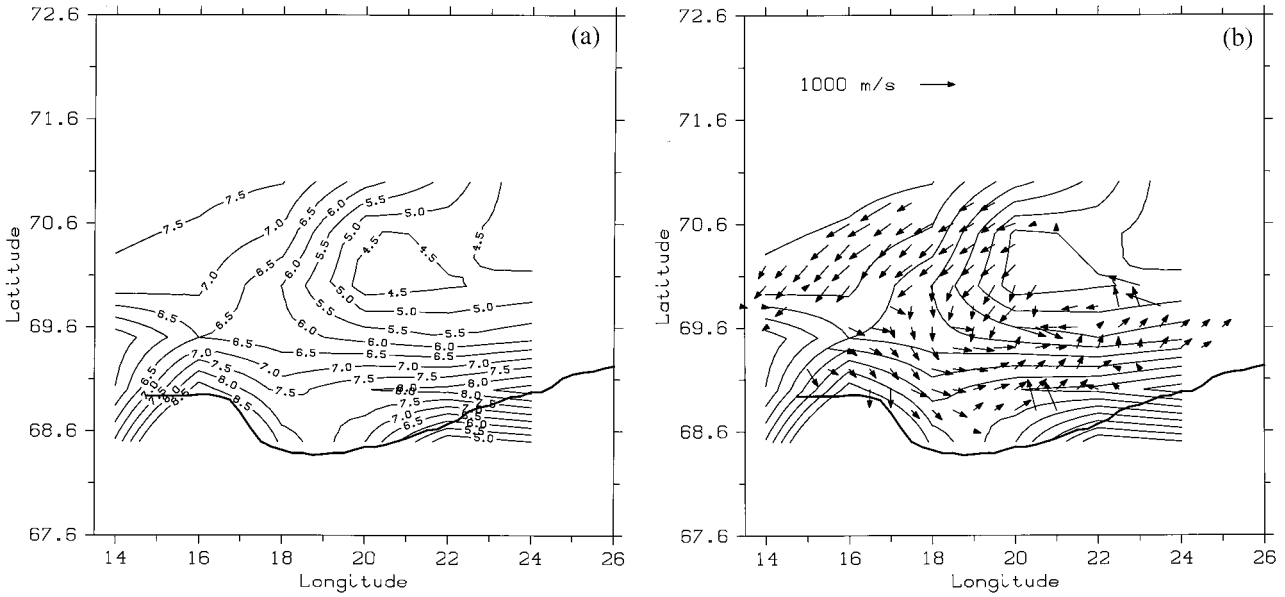

Figure 5. (a) The ionospheric Hall conductance distribution, in siemens, at 2135 UT on January 15, 1980, in geographic coordinates. The lower border of the arc, projected at 100 km altitude, is also shown. A Hall-to-Pedersen conductance ratio of 1.1 is assumed. (b) The same conductance plot with the grid of Scandinavian Twin Auroral Radar Experiment (STARE) plasma flow vectors superimposed.

conductance map reproduces the arc remarkably well. The Pedersen conductance will have exactly the same distribution as Figure 5a, except that values will be reduced by a factor of 1.1 owing to the initial assumption. The results show that even under very quiet geomagnetic conditions ($Kp = 1^+$), auroral precipitation can still produce significant conductivity gradients.

Figure 5b shows the identical conductance plot as in Figure 5a without contour labels but with the STARE plasma flow vectors overlaid. The lower border of the auroral arc is again shown. It is very clear that the region of minimum conductance, centered on about 70.1°N and 21°E, corresponds to the center of the counterclockwise plasma vortex. Equivalently, this region corresponds to the center in the clockwise total current vortex (see Figure 4a). If, as supposed above, this region corresponds to a downward FAC, corresponding to the closure current of the arc, then it would be expected that the conductance be reduced here. This would be consistent with the fact that the downward current would have to be carried by ionospheric thermal electrons accelerated upward. Removal of these electrons with no immediate means of replenishment (e.g., convection) must reduce the local conductivity.

Once the electric field and conductance distributions are known, the FACs can be computed using (4). Figure 6a shows the FAC distribution at 2135 UT on January 15, 1980, in geographic coordinates. The lower border of the arc, projected at 100 km altitude, is also shown. Circles (crosses) correspond to downward (upward) current. The entire region poleward of the arc (~400 × 100 km) corresponds to downward current. The downward FAC region westward of 17°E is not associated with the vortex and probably results from aurora to the northwest outside the field of view (see Figure 1 at 70.8°N), which corresponds to the northwest pointing electric field vectors in this region (see Figure 4b). Downward FAC amplitudes appear to be quite reasonable [*Armstrong et al*., 1975; *de la Beaujardiere et al*., 1977; *Brüning and Goertz*, 1986; *Cahill et al*., 1980; *Evans et al*., 1977; *Marklund et al*., 1982; *Robinson et al*., 1981], with an average of 0.8 μA/m^2 and reaching a maximum value of 1.7 μA/m^2. The downward current region results mostly from the diverging horizontal Pedersen currents (not shown). The auroral arc is expected to correspond to upward FAC carried by precipitating electrons. In the immediate vicinity of the arc the currents appear to be rather small and only partly upward. This lack of a clear signature is attributed to the narrowness of the arc (~20 km), whereas the spatial grid for the method of characteristics is 80 × 50 km. Reducing the spatial grid will achieve no better resolution as, the SMA stations have an average spacing of only ~120 km within the study area. This spacing is justified on the grounds that, given an altitude of maximum ionospheric conductivity at ~100 km above the ground, magnetic field variations with wavelengths <200 km will be strongly attenuated [*Küppers et al*., 1979]. This effectively limits the spatial resolution achieveable to ~100 km. Therefore the "missing" part of the upward FAC due to the arc would have appeared in the grid points equatorward of the southern boundary of the analysis area. Unfortunately, the lack of STARE backscatter equatorward of the arc does not permit any detailed analysis in this region.

The closure current region of the arc has a radius of ~100 km; hence it covers an area of $\pi\ 100^2 \approx 31{,}400$ km^2 with an average current density of 0.8 μA/m^2. Assuming that this corresponds to the length of the arc equatorward of the vortex (17 − 25° longitude), for an arc thickness of 20 km, the area of the arc is 320 × 20 = 6400 km^2. Furthermore, assuming that all of the downward FAC in the plasma vortex closes only with upward FAC in the selected section of the arc, the average upward FAC density in the arc is estimated to be 3.9 μA/m^2. This is consistent with previous observations [*Armstrong et al*., 1975; *de la Beaujardiere et al*., 1977; *Brüning and Goertz*, 1986; *Cahill et al*., 1980; *Evans et al*., 1977; *Marklund et al*., 1982; *Robinson et al*., 1981]. It is concluded that Figure 6a is a realistic representation of the FAC distribution for the downward FACs poleward of the arc.

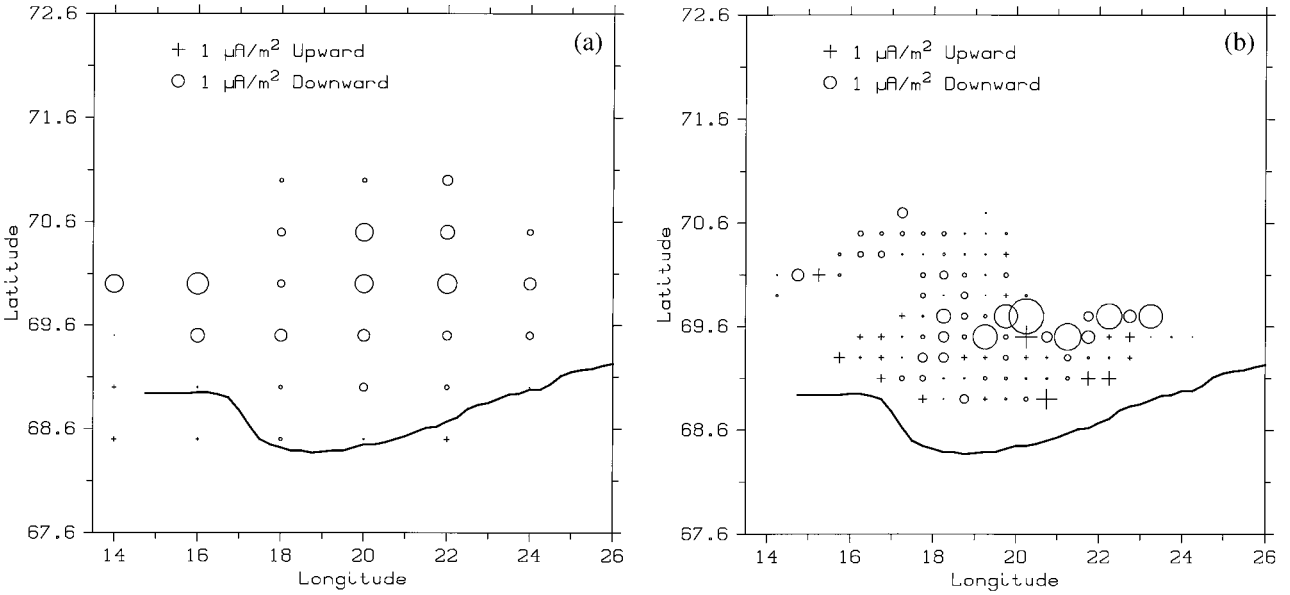

Figure 6. (a) The measured field-aligned current distribution assuming a Hall-to-Pedersen conductance ratio of 1.1. (b) The equivalent field-aligned current distribution, from electric field data only, assuming a constant Pedersen conductance of 1 S. Circles and crosses represent downward and upward magnetic field-aligned currents, respectively. The lower border of the arc, projected at 100 km altitude, is also shown.

In the original study of this event [*Kosch et al*., 1998] an important point was that, for the first time using ground-based data, it was possible to identify the spatial region, associated with an auroral arc, which constituted a closed current sheet pair linked to the magnetosphere. This was possible since the plasma vortex was causally linked to the arc and hence the region of downward FAC was likewise causally linked to the arc, i.e., a region of upward FAC. Figure 6b shows the previous result in the same format as Figure 6a. Figure 6b is a copy of Figure 8 of *Kosch et al*. [1998], reproduced for comparison purposes. This earlier work did not include the SMA data; hence no conductivity measurements were available. Figure 6b was generated by assuming a uniform conductance (1 S) and computing the FACs solely from the divergence of the STARE electric fields. This corresponds to using only the first term of (4). It is seen that a much more localized region (160 × 20 km) of downward current results [*Kosch et al*., 1998] when compared to Figure 6a. The expanded region of downward current in Figure 6a results directly from horizontal conductivity gradients (see Figure 5a), which previously could not be accounted for. The spatial grid used in the method of characteristics (50 × 80 km), which is limited by the SMA data as explained earlier, could also contribute to the smearing out of the region of downward current. However, this is a secondary effect. In Figure 6b the grid size is much smaller (20 × 20 km) because it is limited by the STARE data only. Had there been no horizontal conductivity gradients, Figures 6a and 6b would be identical except for a simple scaling factor. Auroral precipitation produces significant horizontal conductivity gradients, which cannot be ignored when computing FACs.

It is seen that the conductance gradients have a significant effect on the distribution of the closure current associated with the arc. Although it seems clear that the auroral arc can be considered to be an upward FAC sheet localized in space, the downward FAC area, which constitutes the return current in this event, is centered on the apex of the plasma vortex with a radius of ~100 km. This is considerably larger than the return current area found in the previous study [*Kosch et al*., 1998], the increase being approximately an order of magnitude. Hence ionospheric conductance gradients tend to broaden the downward FAC region and so decrease the FAC area density. The larger analysis grid size imposed by the SMA data may also contribute in a small way to the broadening of the downward FAC region.

3. Black Aurora

Black aurora have been reviewed by *Kosch et al*. [1998]. *Marklund et al*. [1997] describe Freja satellite observations that have been associated with black aurorae, although there were no direct optical observations. There are a number of striking simularities with the event studied here. These include diverging electric fields in a region of very low electron precipitation (i.e., no auroral emission): this region has a depleted conductivity and contains downward FAC, which is associated with the upward acceleration of low-energy ionospheric electrons. The positive counterpart, namely, the auroral arc, was adjacent to the presumed black aurora. Many of their observations occurred near magnetic midnight, similar to our observation. For the same event studied here, *Kosch et al*. [1998] found strong circumstantial evidence that the plasma vortex was colocated with a black aurora. Unfortunately, this could not be confirmed conclusively from the all-sky optical data. However, *Schoute-Vanneck et al*. [1990] found a total of 186 black aurorae from the same data set only 4 min after the event described here. These were observed with a small field of view TV camera centered on the zenith over Skibotn. Unfortunately, this camera did not cover the region of sky where the plasma vortex occurred. There are some differences also. We do not observe the intense small-scale (1–2 km) electric fields (150–300 mV/m) described by *Marklund et al*. [1997]. However, this may simply be due to our limited spatial resolution, resulting in

averaging. We conclude that the plasma vortex was probably colocated with a black aurora, which we associate with the sudden brightening of the auroral arc.

4. Conclusions

At a geomagnetically quiet time ($Kp = 1^+$) an auroral arc optically brightens following the passage of an eastward surge. This has been causally related to an ionospheric plasma vortex poleward of the arc in which STARE plasma drift vectors rotate counterclockwise [*Kosch et al*., 1998]. Combining STARE equivalent electric fields with the SMA equivalent currents allows the conductance distribution to be calculated and hence the real three-dimensional currents to be computed. The entire plasma vortex coincides with a region of downward magnetic field-aligned current (FAC), i.e., the closure current for the upward FAC above the arc. The plasma vortex center coincides with a minimum in conductance, which is expected from the upward flow of thermal electrons. The closure current region of the arc covers approximately $\pi\ 100^2 \approx 31{,}400\ \text{km}^2$, which is much more extensive in area than previously reported (3200 km^2) [*Kosch et al*., 1998]. This results directly from horizontal conductivity gradients that previously could not be accounted for. Even during very quiet geomagnetic conditions, conductance gradients, resulting from auroral precipitation, cannot be neglected when computing FACs. There is circumstantial evidence that the plasma vortex may be colocated with a black aurora.

This study has used data from a single point in time: a snapshot. We speculate that the spatial extent of the closure current of an arc may develop with time. For example, assuming that the downward closure FAC is somewhat spatially localized, it would be expected that the thermal electrons, which carry this current, would be accelerated upward, thereby reducing the local conductivity. Either conductivity gradients would be created or existing ones would be enhanced. Such a situation would automatically result in a spreading out of the closure current region because the horizontal currents feeding the closure FAC have to cross regions of changing conductivity; that is, the last two terms of (4) are increasingly invoked with time. The changing spatial morphology of arc-associated closure currents will be the topic of future work.

Acknowledgments. The STARE radars are operated by the Max-Planck-Institut für Aeronomie in cooperation with ELAB, the Norwegian Technical University (Trondheim), and the Finnish Meteorological Institute (Helsinki). The assistance of E. Nielsen in processing the STARE data as well as K.-H. Glassmeier and B. Inhester in analyzing the SMA data is gratefully acknowledged. The work of O.A. was supported by a DAAD postdoctoral fellowship HSP III financed by the German Federal Ministry for Research and Technology.

Michel Blanc thanks Göran Marklund and Robert M. Robinson for their assistance in evaluating this paper.

References

Aikio, A. T., H. J. Opgenoorth, M. A. L. Persson, and K. U. Kaila, Ground-based measurements of an arc-associated electric field, *J. Atmos. Terr. Phys*., *55*, 797, 1993.

Amm, O., Direct determination of the local ionospheric Hall conductance distribution from two-dimensional electric and magnetic field data: Application of the method using models of typical ionospheric electrodynamic situations, *J. Geophys. Res*., *100*, 21,473, 1995.

Amm, O., Ionospheric elementary current systems in spherical coordinates and their application, *J. Geomagn. Geoelectr*., *49*, 947, 1997.

Amm, O., Method of characteristics in spherical geometry applied to a Harang Discontinuity situation, *Ann. Geophys*., *16*, 413, 1998.

Amm, O., and A. Viljanen, Ionospheric disturbance magnetic field continuation from the ground to the ionosphere using spherical elementary current systems, *Earth Planets Space*, *51*, 431, 1999.

Armstrong, J. C., S.-I. Akasofu, and G. Rostoker, A comparison of satellite observations of Birkeland currents with ground observations of visible aurora and ionospheric currents, *J. Geophys. Res*., *80*, 575, 1975.

Aruliah, A. L., D. Rees, and T. J. Fuller-Rowell, The combined effect of solar and geomagnetic activity on high latitude thermospheric neutral winds, part I, Observations, *J. Atmos. Terr. Phys*., *53*, 467, 1991.

Baumjohann, W., Ionospheric and field-aligned current systems in the auroral zone: A concise review, *Adv. Space Res*., *2*(10), 55, 1983.

Baumjohann, W., R. J. Pellinen, H. J. Opgenoorth, and E. Nielsen, Joint two-dimensional observations of ground magnetic and ionsopheric electric fields associated with auroral zone currents: Current systems associated with local auroral break-ups, *Planet. Space Sci*., *29*, 431, 1981.

Brüning, K., and C. K. Goertz, Dynamics of a discrete auroral arc, *J. Geophys. Res*., *91*, 7057, 1986.

Cahill, L. J., R. A. Greenwald, and E. Nielsen, Auroral radar and rocket double probe observations of the electric field across the Harang Discontinuity, *Geophys. Res. Lett*., *5*, 687, 1978.

Cahill, L. J., Jr., R. L. Arnoldy, and W. L. Taylor, Rocket observations at the northern edge of the eastward electrojet, *J. Geophys. Res*., *85*, 3407, 1980.

Cierpka, K., M. Kosch, M. Rietveld, K. Schlegel, and T. Hagfors, Ion-neutral coupling in the high-latitude F-layer from incoherent scatter and Fabry-Perot interferometer measurements, *Ann. Geophys*., in press, 2000.

de la Beaujardiere, O., R. Vondrak, and M. Baron, Radar observations of electric fields and currents associated with auroral arcs, *J. Geophys. Res*., *82*, 5051, 1977.

de la Beaujardiere, O., R. Vondrak, R. Heelis, W. Hanson, and R. Hoffman, Auroral arc electrodynamic parameters measured by AE-C and the Chatanika Radar, *J. Geophys. Res*., *86*, 4671, 1981.

Evans, D. S., N. C. Maynard, J. Troim, T. Jacobsen, and A. Egeland, Auroral vector electric field and particle comparisons, 2, Electrodynamics of an arc, *J. Geophys. Res*., *82*, 2235, 1977.

Fejer, B. J., and M. C. Kelley, Ionospheric irregularities, *Rev. Geophys*., *18*, 401, 1980.

Folkestad, K., T. Hagfors, and S. Westerlund, EISCAT: An updated description of technical characteristics and operational capabilities, *Radio Sci*., *18*, 867, 1983.

Fukushima, N., Generalized theorem of no ground magnetic effect of vertical currents connected with Pedersen currents in the uniform conducting ionosphere, *Rep. Ionos. Space Res. Jpn*., *30*, 35, 1976.

Greenwald, R. A., W. Weiss, E. Nielsen, and N. R. Thomson, STARE: A new radar auroral backscatter experiment in northern Scandinavia, *Radio Sci*., *13*, 1021, 1978.

Horwitz, J. L., J. R. Doupnik, and P. M. Banks, Chatanika radar observations of the latitudinal distributions of auroral zone electric fields, conductivities, and currents, *J. Geophys. Res*., *83*, 1463, 1978.

Inhester, B., W. Baumjohann, R. A. Greenwald, and E. Nielsen, Joint two-dimensional observations of ground magnetic and ionsopheric electric fields associated with auroral zone currents, 3, Auroral zone currents during the passage of a westward travelling surge, *J. Geophys*., *49*, 155, 1981.

Inhester, B., J. Untiedt, M. Segatz, and M. Kürschner, Direct determination of the local ionospheric Hall conductance distribution from two-dimensional electric and magnetic field data, *J. Geophys. Res*., *97*, 4073, 1992.

Kamide, Y., and S.-I. Akasofu, The location of the field-aligned currents with respect to discrete arcs, *J. Geophys. Res*., *81*, 3999, 1976a.

Kamide, Y., and S.-I. Akasofu, The auroral electrojet and field-aligned current, *Planet. Space Sci*., *24*, 203, 1976b.

Killeen, T. L., and R. G. Roble, An analysis of the high-latitude thermosphere wind pattern calculated by a thermospheric general circulation model, 1, Momentum forcing, *J. Geophys. Res*., *89*, 7509, 1984.

Killeen, T. L., and R. G. Roble, Thermosphere dynamics: Contributions from the first 5 years of the Dynamics Explorer program, *Rev. Geophys*., *26*, 329, 1988.

Killeen, T. L., P. B. Hays, G. R. Carignan, R. A. Heelis, W. B. Hanson,

N. W. Spencer, and L. H. Brace, Ion-neutral coupling in the high-latitude F region: Evaluation of ion heating terms from Dynamics Explorer 2, *J. Geophys. Res*., *89*, 7495, 1984.

Korth, A., G. Kremser, and B. Wilken, Observations of substorm-associated particle flux variations at $6 < L < 8$ with GEOS-1, *Space Sci. Rev*., *22*, 501, 1978.

Kosch, M. J., M. W. J. Scourfield, and E. Nielsen, A self-consistent explanation for a plasma flow vortex associated with the brightening of an auroral arc, *J. Geophys. Res*., *103*, 29,383, 1998.

Kosch, M. J., et al., A comparison of thermospheric winds and temperatures from Fabry-Perot interferometer and EISCAT radar measurements with models, *Adv. Space Res*., *26*(6), 979, 2000.

Küppers, F., J. Untiedt, W. Baumjohann, K. Lange, and A. G. Jones, A two-dimensional magnetometer array for ground-based observations of auroral zone electric currents during the International Magnetospheric Study (IMS), *J. Geophys*., *46*, 429, 1979.

Lester, M., J. A. Davies, and T. S. Virdi, High-latitude Hall and Pedersen conductances during substorm activity in the SUNDIAL-ATLAS campaign, *J. Geophys. Res*., *101*, 26,719, 1996.

Lewis, R. V., P. J. S. Williams, G. O. L. Jones, H. J. Opgenoorth, and M. A. L. Persson, The electrodynamics of a drifting arc, *Ann. Geophys*., *12*, 478, 1994.

Marklund, G., Auroral arc classification scheme based on the observed arc-associated electric field pattern, *Planet. Space Sci*., *32*, 193, 1984.

Marklund, G., I. Sandahl, and H. J. Opgenoorth, A study of the dynamics of a discrete auroral arc, *Planet. Space Sci*., *30*, 179, 1982.

Marklund, G., T. Karlsson, and J. Clemmons, On low-altitude particle acceleration and intense electric fields and their relationship to black aurora, *J. Geophys. Res*., *102*, 17,509, 1997.

McCormac, F. G., T. L. Killeen, J. P. Thayer, G. Hernandez, C. R. Tschan, N. W. Spencer, and J.-J. Ponthieu, Circulation of the polar thermosphere during geomagnetically quiet and active times as observed by Dynamics Explorer 2, *J. Geophys. Res*., *92*, 10,133, 1987.

Mende, S. B., R. H. Eather, M. H. Rees, R. R. Vondrak, and R. M. Robinson, Optical mapping of ionospheric conductances, *J. Geophys. Res*., *89*, 1755, 1984.

Nielsen, E., and A. Greenwald, Electron flow and visual aurora at the Harang Discontinuity, *J. Geophys. Res*., *84*, 4189, 1979.

Opgenoorth, H. J., R. J. Pellinen, W. Baumjohann, E. Nielsen, G. Marklund, and L. Eliasson, Three-dimensional current flow and particle precipitation in a westward travelling surge (observed during the barium-GEOS rocket experiment), *J. Geophys. Res*., *88*, 3138, 1983a.

Opgenoorth, H. J., J. Oksman, K. U. Kaila, E. Nielsen, and W. Baumjohann, Characteristics of eastward drifting omega bands in the morning sector of the auroral oval, *J. Geophys. Res*., *88*, 9171, 1983b.

Opgenoorth, H. J., I. Häggström, P. J. S. Williams, and G. O. L. Jones, Regions of strongly enhanced perpendicular electric fields adjacent to auroral arcs, *J. Atmos. Terr. Phys*., *52*, 449, 1990.

Robinson, R. M., E. A. Bering, R. R. Vondrak, H. R. Anderson, and P. A. Cloutier, Simultaneous rocket and radar measurements of currents in an auroral arc, *J. Geophys. Res*., *86*, 7703, 1981.

Robinson, R., R. Vondrak, J. Craven, L. Frank, and K. Miller, A comparison of ionospheric conductances and auroral luminosities observed simultaneously with the Chatanika Radar and the DE1 Auroral Imagers, *J. Geophys. Res*., *94*, 5382, 1989.

Sato, M., Y. Kamide, A. D. Richmond, A. Brekke, and S. Nozawa, Regional estimation of electric fields and currents in the polar ionosphere, *Geophys. Res. Lett*., *22*, 283, 1995.

Schlegel, K., Auroral zone E-region conductivities during solar minimum derived from EISCAT data, *Ann. Geophys*., *6*, 129, 1988.

Schoute-Vanneck, H., M. W. J. Scourfield, and E. Nielsen, Drifting black aurorae?, *J. Geophys. Res*., *95*, 241, 1990.

Sofko, G. J., R. Greenwald, and W. Bristow, Direct determination of large-scale magnetospheric field-aligned currents with SuperDARN, *Geophys. Res. Lett*., *22*, 2041, 1995.

Stiles, G. S., J. C. Foster, and J. R. Doupnik, Prolonged radar observations of an auroral arc, *J. Geophys. Res*., *85*, 1223, 1980.

Timofeev, E. E., M. K. Vallinkoski, T. V. Jozelova, A. G. Yahnin, and R. J. Pellinen, Systematics of arc-associated electric fields and currents as inferred from radar backscatter measurements, *J. Geophys*., *61*, 122, 1987.

Tsunoda, R. T., R. I. Presnell, and T. A. Potemra, The spatial relationship between the evening radar aurora and field-aligned currents, *J. Geophys. Res*., *81*, 3791, 1976.

Untiedt, J., and W. Baumjohann, Studies of polar current systems using the IMS Scandinavian magnetometer array, *Space Sci. Rev*., *63*, 245, 1993.

Valladares, C. E., and H. C. Carlson Jr., The electrodynamics, thermal and energetic character of intense Sun-aligned arcs in the polar cap, *J. Geophys. Res*., *96*, 1379, 1991.

Vickrey, J. F., R. R. Vondrak, and S. J. Matthews, The diurnal and latitudinal variation of auroral zone ionospheric conductivity, *J. Geophys. Res*., *86*, 65, 1981.

Ziesolleck, C. H., W. Baumjohann, K. Brüning, C. W. Carlsson, and R. I. Bush, Comparison of height-integrated current densities derived from ground-based magnetometer and rocket-borne observations during the Porcupine F3 and F4 flights, *J. Geophys. Res*., *88*, 8063, 1983.

O. Amm, Finnish Meteorological Institute, 00101 Helsinki, Finland.

M. J. Kosch, Max-Planck-Institut für Aeronomie, Max-Planck Strasse 2, 37191 Katlenburg-Lindau, Germany. (kosch@linmpi.mpg.de)

M. W. J. Scourfield, Space Physics Research Institute, University of Natal, 4001 Durban, South Africa.

(Received January 18, 2000; revised May 4, 2000;
accepted June 18, 2000.)